www.sciencemag.org/content/359/6383/aaq0939/suppl/DC1

Supplementary Materials for

Structure of the nucleotide exchange factor eIF2B reveals mechanism of memory-enhancing molecule

Jordan C. Tsai, Lakshmi E. Miller-Vedam, Aditya A. Anand, Priyadarshini Jaishankar, Henry C. Nguyen, Adam R. Renslo, Adam Frost,* Peter Walter*

*Corresponding author. Email: peter@walterlab.ucsf.edu (P.W.); adam.frost@ucsf.edu (A.F.)

Published 30 March 2018, *Science* **359**, eaaq0939 (2018)
DOI: 10.1126/science.aaq0939

This PDF file includes:

Additional Materials and Methods

ISRIB-A19*(R,R)* and *(S,S)* synthesis & validation

(2S)-2-(4-chlorophenoxy)propanoic acid was purchased from Enamine. Reagents and solvents were purchased from Sigma- Aldrich, Acros or TCI America and used as received unless otherwise indicated. Flash column chromatography was carried out using a Biotage Isolera Four system and Silia*Sep* silica gel cartridges from Silicycle. ^{1}H NMR spectra were recorded on a Varian INOVA-400 400MHz spectrometer. Chemical shifts are reported in δ units (ppm) relative to residual NMR solvent peaks. Coupling constants (*J*) are reported in hertz (Hz). Characterization data are reported as follows: chemical shift, multiplicity (s=singlet, d=doublet, t=triplet, q=quartet, br=broad, m=multiplet), coupling constants, number of protons, mass to charge ratio. LC/MS analyses were performed on a Waters Micromass ZQ/Waters 2795 Separation Module/Waters 2996 Photodiode Array Detector/Waters 2424 Evaporative Light Scattering Detector system. Separations were carried out on XTerra® MS C_{18} 5µm 4.6x50mm column at ambient temperature using a mobile phase of water-methanol containing 0.1% formic acid.

Synthesis of (2*S*)-2-(4-Chlorophenoxy)-N-[(1r,4r)-4-[(2S)-2-(4-chlorophenoxy)propanamido]cyclohexyl]propanamide (ISRIB-A19*(S,S)*):

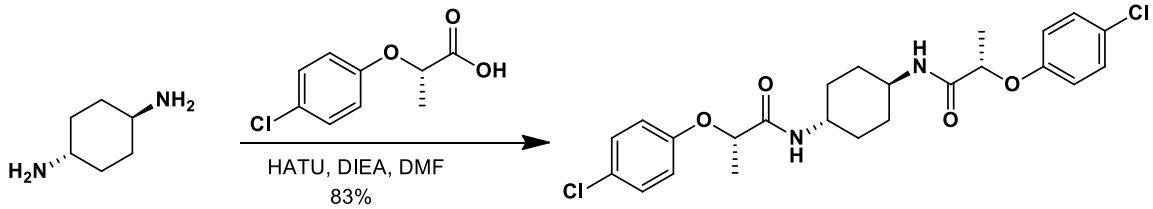

To a solution of the (2*S*)-2-(4-chlorophenoxy)propanoic acid (0.176 g, 0.88 mmol) in *N,N*-dimethylformamide (4 ml), was added HATU (0.35 g, 0.88 mmol), *trans*-1,4-diaminocyclohexane (0.05 g, 0.44 mmol), and *N,N*-diisopropylethylamine (0.3 ml, 1.76 mmol). The mixture was stirred at ambient temperature until the reaction was judged complete by LC/MS. The reaction mixture was then filtered and the collected material washed with diethyl ether, water, and then dried to obtain 175 mg (83%) of the title compound as a white solid. ^{1}H NMR (400 MHz, d_6-DMSO) δ 7.96 (d, J = 8 Hz, 2H), 7.30-7.34 (m, 4H), 6.89-6.93 (m, 4H), 4.63 (q, J = 6.6 Hz, 2H), 3.48 (br.s, 2H), 1.73 (d, J = 7.3 Hz, 2H), 1.64 (d, J = 7.3 Hz, 2H), 1.40(d, J = 6.6 Hz, 6H), 1.23-1.33 (m, 4H); 13C NMR (100 MHz, $CDCl_3$) δ 170.40, 156.85, 129.65, 125.17, 117.41, 74.31, 47.33, 31.16, 19.10; LCMS *m/z* 479 (MH+).

Synthesis of ethyl (2*R*)-2-(4-chlorophenoxy)propanoate:

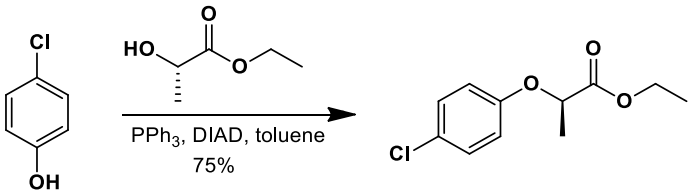

To a cooled (-20° C) solution of ethyl (2*S*)-2-hydroxypropanoate (0.330 g, 2.8 mmol), 4-chlorophenol (0.359 g, 2.8 mmol) and triphenylphosphine (0.733 g, 2.8 mmol, 1.0 equiv.) in toluene was added diisopropyl azodicarboxylate (0.550 ml, 2.8 mmol). The mixture was stirred at -20° C for an hour and then at ambient temperature for 24 hours. The reaction mixture was concentrated *in vacuo* to remove the toluene solvent. To the resulting residue was added hexanes and the precipitate that formed was filtered off. The filtrate was concentrated *in vacuo* and purified by flash column chromatography (25 g, 0-10% EA/hex) to obtain 0.48 g (75%) of the product as a yellow oil. ^{1}H NMR (400 MHz, $CDCl_3$) δ 7.21-7.26 (m, 2H), 6.80-6.84 (m, 2H), 4.71 (q, J = 6.8 Hz, 1H), 4.20-4.25 (m, 2H), 1.62 (d, J = 6.8 Hz, 3H), 1.26 (t, J = 7.2 Hz, 3H); LCMS *m/z* 228 (MH+).

Synthesis of (2R)-2-(4-Chlorophenoxy)-N-[(1r,4r)-4-[(2R)-2-(4-chlorophenoxy)propanamido]cyclohexyl]propanamide (ISRIB-A19*(R,R)*):

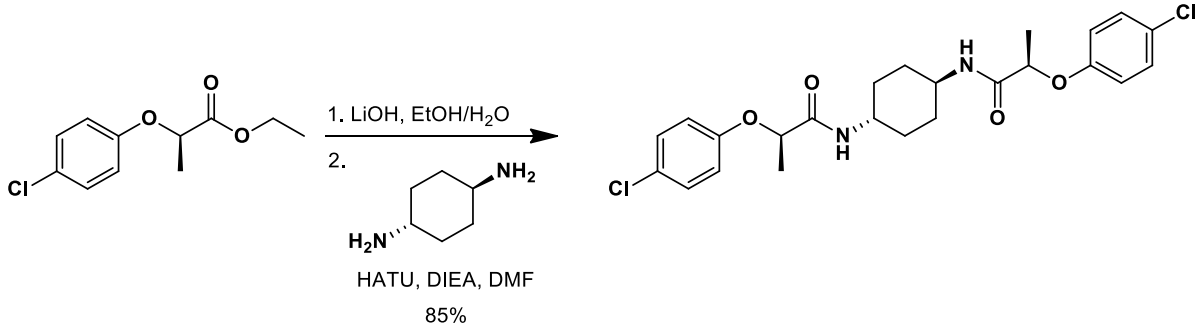

To a solution of ethyl (2R)-2-(4-chlorophenoxy)propanoate (0.150 g, 0.7 mmol) in 2:1 mixture of ethanol-water (6 ml) was added 1 M aqueous lithium hydroxide solution (1.312 ml, 1.3 mmol). The mixture was stirred at ambient temperature for 24 h. The reaction mixture was concentrated *in vacuo* to remove ethanol, diluted with water and adjusted to pH 2 with 1 N aqueous hydrochloric acid solution. The mixture was extracted with ethyl acetate. The organic extracts were washed with brine, dried over magnesium sulfate and concentrated to obtain 123 mg of (2R)-2-(4-chlorophenoxy)propanoic acid as a white solid. This material was used directly in the next reaction.

To a solution of the (2R)-2-(4-chlorophenoxy)propanoic acid (0.1 g, 0.5 mmol) in *N,N*-dimethylformamide (2 ml), was added HATU (0.2 g, 0.525 mmol), *trans*-1,4-diaminocyclohexane (0.028 g, 0.25 mmol), and *N,N*-diisopropylethylamine (0.174 ml, 1.0 mmol). The mixture was stirred at ambient temperature until the reaction was judged complete by LC/MS. The reaction mixture was filtered and the collected material was washed with diethyl ether, water, and then dried to obtain 100 mg (85%) of the title compound as a white solid. ^{1}H NMR (400 MHz, d_6-DMSO) δ 7.96 (d, J = 8.3 Hz, 2H),

7.30-7.34 (m, 4H), 6.88-6.92 (m, 4H), 4.63 (q, *J* = 6.5 Hz, 2H), 3.49 (br.s, 2H), 1.73 (d, *J* = 8.3 Hz, 2H), 1.64 (d, *J* = 7.3 Hz, 2H), 1.44 (d, *J* = 6.6 Hz, 6H), 1.22-1.30 (m, 4H); LCMS *m/z* 479 (MH+).

Confirmation of inversion of configuration in preparation of intermediates for ISRIB-A19*(R,R)* synthesis.

To confirm inversion of stereochemical configuration during the preparation of ethyl (2*R*)-2-(4-chlorophenoxy)propanoate, the (2*S*)-2-(4-chlorophenoxy)propanoic acid and (2*R*)-2-(4-chlorophenoxy)propanoic acid used in the preparation of ISRIB-A19*(S,S)* and ISRIB-A19*(R,R)*, respectively, were coupled to (*R*)-(+)-alpha-methylbenzylamine as detailed below. The resulting amides were found to be single and distinct diastereoisomers, confirming the enantiomeric relationship of the propanoic acids and accordingly of ISRIB-A19*(R,R) and* ISRIB-A19*(R,R)*.

Synthesis of (2*S*)-2-(4-chlorophenoxy)-N-[(1*R*)-1-phenylethyl]propanamide:

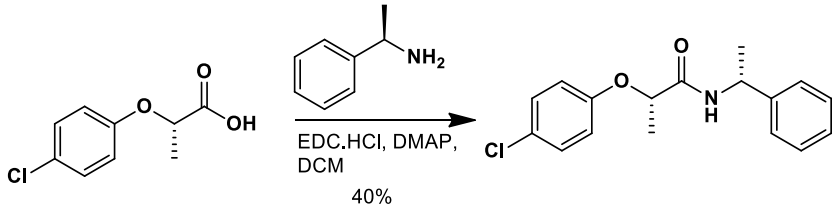

To a solution of (2*S*)-2-(4-chlorophenoxy)propanoic acid (0.050 g, 0.2 mmol) in CH_2Cl_2 (3 ml) was added 1-(3-dimethylaminopropyl)-3-ethylcarbodiimide hydrochloride (0.048 g, 0.3 mmol), 4-dimethylaminopyridine (0.003 g, 0.025 mmol), and finally (*R*)-(+)-alpha-methylbenzylamine (0.032 ml, 0.2 mmol). The mixture was stirred at ambient temperature for 24 h. The reaction mixture was then washed with saturated aqueous ammonium chloride, water and brine. The organic layer was separated, dried over magnesium sulfate, filtered and concentrated. The crude product was purified by flash column chromatography (0-50% EtOAc/hexanes) to yield 30 mg (40%) of the title compound as a white solid. ^{1}H NMR (400 MHz, $CDCl_3$) δ 7.36-7.40 (m, 2H), 7.27-7.32 (m, 5H), 6.86-6.90 (m, 2H), 6.59 (d, *J* = 7.8 Hz, 1H), 5.15-5.20 (m, 1H), 4.66 (q, *J* = 6.8 Hz, 1H), 1.56 (d, *J* = 6.6 Hz, 3H), 1.43 (d, *J* = 6.8 Hz, 3H); 13C NMR (100 MHz, $CDCl_3$) δ 170.84, 155.49, 142.68, 129.79, 127.53, 127.12, 126.05, 116.87, 75.59, 48.27, 21.63, 18.68; LCMS *m/z* 304 (MH+).

Synthesis of (2*R*)-2-(4-chlorophenoxy)-N-[(1*R*)-1-phenylethyl]propanamide:

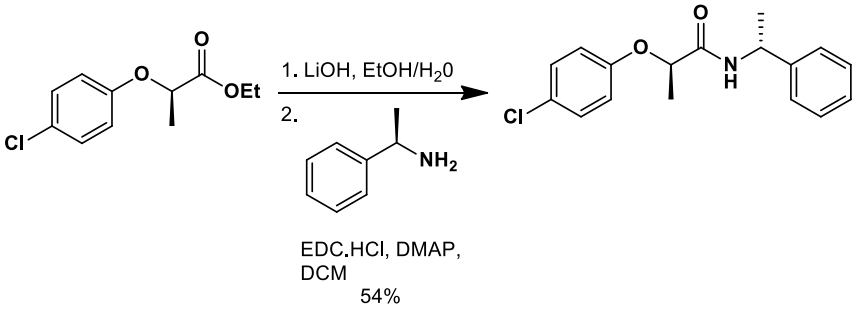

To a solution of ethyl (2*R*)-2-(4-chlorophenoxy)propanoate (0.1 g, 0.44 mmol) in a 2:1 mixture of ethanol-water (6 ml) was added 1 M aqueous lithium hydroxide solution (0.88 ml, 0.88 mmol). The mixture was stirred at ambient temperature for 18 h. The reaction mixture was concentrated *in vacuo* to remove ethanol, diluted with water and adjusted to pH 2 with 1N aqueous hydrochloric acid solution. The mixture was extracted with ethyl acetate. The organic extracts were washed with brine, dried over magnesium sulfate and concentrated to obtain 85 mg of (2*R*)-2-(4-chlorophenoxy)propanoic acid as a white solid. This material was used directly in the next step.

To a solution of the (2*R*)-2-(4-chlorophenoxy)propanoic acid (0.085 g, 0.42 mmol) in CH_2Cl_2 (5 ml) was added 1-(3-dimethylaminopropyl)-3-ethylcarbodiimide hydrochloride (0.082 g, 0.43 mmol), 4-dimethylaminopyridine (0.005 g, 0.042 mmol), and finally (*R*)-(+)-alpha-methylbenzylamine (0.054 ml, 0.42 mmol). The mixture was stirred at ambient temperature for 24 hours. The reaction mixture was then washed with saturated aqueous ammonium chloride, water and brine. The organic layer was separated, dried over magnesium sulfate, filtered and concentrated. The crude product was purified by flash column chromatography (0-50% EtOAc/hexanes) to yield 70 mg (54%) of the title compound as a white solid. ^{1}H NMR (400 MHz, $CDCl_3$) δ 7.21-7.26 (m, 5H), 7.09-7.11 (m, 2H), 6.79-6.83 (m, 2H), 6.56-6.58 (m, 1H), 5.10-5.18 (m, 1H), 4.63 (q, J = 6.7 Hz, 1H), 1.61 (d, J = 6.6 Hz, 3H), 1.52 (d, J = 7.1 Hz, 3H); 13C NMR (100 MHz, $CDCl_3$) δ 170.96, 155.46, 142.67, 129.67, 128.58, 127.36, 127.08, 125.91, 116.89, 75.50, 48.30, 21.80, 18.77; LCMS *m/z* 304 (MH+).

10/12/2017 12:32:42 PM
(2S)-2-(4-Chlorophenoxy)-N-[(1r,4r)-4-[(2S)-2-(4-chlorophenoxy)propanamido]cyclohexyl]propanamide (1014817)

Acquisition Time (sec)	4.1069	***Comment***	Z116098_0411 (PA BBO 400S1 BBF-H-D-05 Z SP)			***Date***	15 Feb 2017 14:24:00
Date Stamp	15 Feb 2017 14:24:00			***File Name***	C:\Users\priya\Desktop\NMRSpectra\NMR#149\149FTD's\PJ149-10\1\fid		
Frequency (MHz)	399.54	***Nucleus***	1H	***Number of Transients***	16	***Origin***	spect
Original Points Count	32768	***Owner***	SMDC_A	***Points Count***	32768	***Pulse Sequence***	zg30
Receiver Gain	166.07	***SW(cyclical) (Hz)***	7978.72	***Solvent***	DMSO-d6	***Spectrum Offset (Hz)***	2467.1362
Spectrum Type	STANDARD	***Sweep Width (Hz)***	7978.48	***Temperature (degree C)***	24.996		

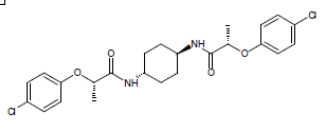

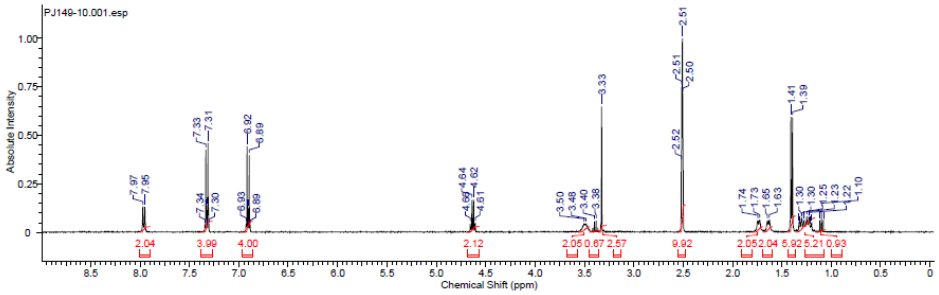

10/12/2017 12:35:49 PM
(2S)-2-(4-Chlorophenoxy)-N-[(1r,4r)-4-[(2S)-2-(4-chlorophenoxy)propanamido]cyclohexyl]propanamide (1014817)

Acquisition Time (sec)	1.3631	***Comment***	Z116098_0411 (PA BBO 400S1 BBF-H-D-05 Z SP)			***Date***	12 Oct 2017 09:42:40
Date Stamp	12 Oct 2017 09:42:40			***File Name***	C:\Users\priya\Desktop\NMRSpectra\NMR#149\149FTD's\PJ149-10C13\1\fid		
Frequency (MHz)	100.46	***Nucleus***	13C	***Number of Transients***	167	***Origin***	spect
Original Points Count	32768	***Owner***	SMDC_A	***Points Count***	32768	***Pulse Sequence***	zgpg30
Receiver Gain	208.51	***SW(cyclical) (Hz)***	24038.46	***Solvent***	DMSO-d6	***Spectrum Offset (Hz)***	10046.3408
Spectrum Type	STANDARD	***Sweep Width (Hz)***	24037.73	***Temperature (degree C)***	24.996		

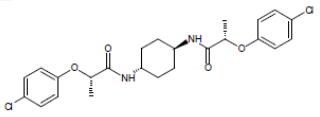

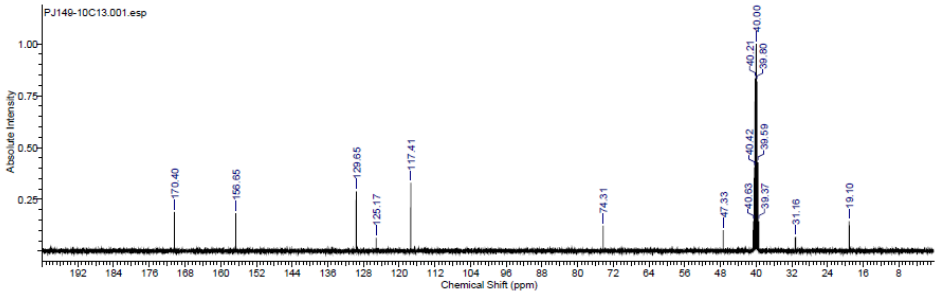

10/12/2017 12:38:37 PM
(2R)-2-(4-Chlorophenoxy)-N-[(1r,4r)-4-[(2R)-2-(4-chlorophenoxy)propanamido]cyclohexyl]propanamide (1014869)

Acquisition Time (sec)	4.1069	*Comment*	Z116098_0411 (PA BBO 400S1 BBF-H-D-05 Z SP)			*Date*	15 Mar 2017 09:23:28
Date Stamp	15 Mar 2017 09:23:28			*File Name*	C:\Users\priya\Desktop\NMRSpectra\NMR#149\149FTD's\PJ149-27\1\fid		
Frequency (MHz)	399.54	*Nucleus*	1H	*Number of Transients*	16	*Origin*	spect
Original Points Count	32768	*Owner*	SMDC_A	*Points Count*	32768	*Pulse Sequence*	zg30
Receiver Gain	185.41	*SW(cyclical) (Hz)*	7978.72	*Solvent*	DMSO-d6	*Spectrum Offset (Hz)*	2467.1362
Spectrum Type	STANDARD	*Sweep Width (Hz)*	7978.48	*Temperature (degree C)*	25.002		

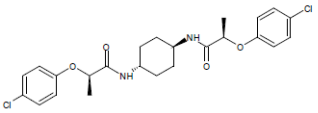

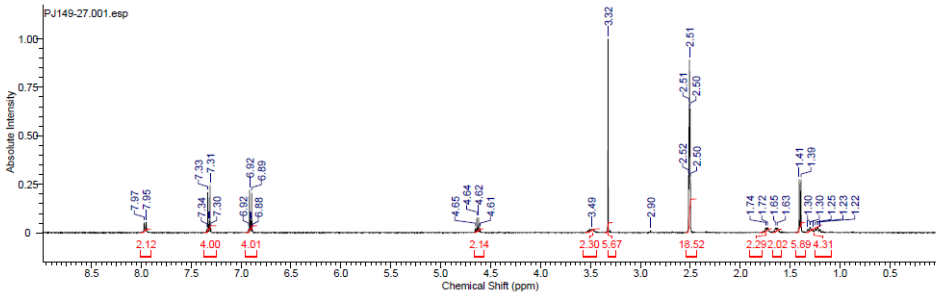

10/10/2017 11:16:06 AM
(2S)-2-(4-chlorophenoxy)-N-[(1R)-1-phenylethyl]propanamide

Acquisition Time (sec)	4.1069	*Comment*	Z116098_0411 (PA BBO 400S1 BBF-H-D-05 Z SP)			*Date*	25 Sep 2017 10:12:32
Date Stamp	25 Sep 2017 10:12:32			*File Name*	C:\Users\priya\Desktop\NMRSpectra\NMR#149\149FTD's\PJ149-127\1\fid		
Frequency (MHz)	399.54	*Nucleus*	1H	*Number of Transients*	16	*Origin*	spect
Original Points Count	32768	*Owner*	SMDC_A	*Points Count*	32768	*Pulse Sequence*	zg30
Receiver Gain	74.50	*SW(cyclical) (Hz)*	7978.72	*Solvent*	CHLOROFORM-d		
Spectrum Offset (Hz)	2467.1362	*Spectrum Type*	STANDARD	*Sweep Width (Hz)*	7978.48	*Temperature (degree C)*	25.002

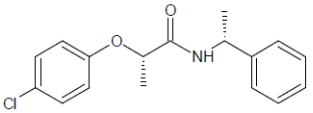

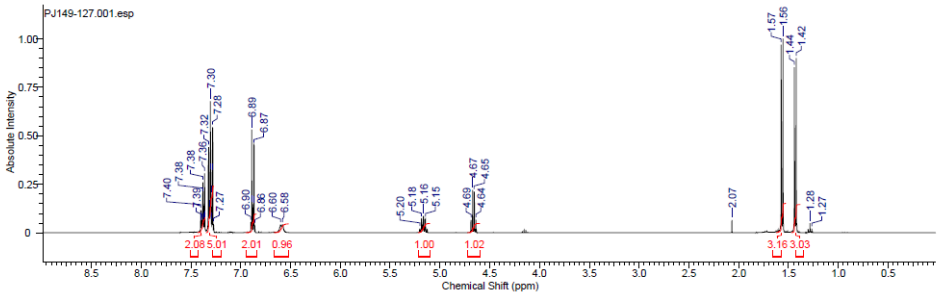

10/12/2017 11:22:58 AM
(2S)-2-(4-chlorophenoxy)-N-[(1R)-1-phenylethyl]propanamide

Acquisition Time (sec)	1.3631	*Comment*	Z116098_0411 (PA BBO 400S1 BBF-H-D-05 Z SP)	*Date*	25 Sep 2017 10:16:48
Date Stamp	25 Sep 2017 10:16:48		*File Name*	C:\Users\priya\Desktop\NMRSpectra\NMR#149\149FTD's\PJ149-127C13\1\fid	
Frequency (MHz)	100.46	*Nucleus*	13C	*Number of Transients*	130	*Origin*	spect
Original Points Count	32768	*Owner*	SMDC_A	*Points Count*	32768	*Pulse Sequence*	zgpg30
Receiver Gain	208.51	*SW(cyclical) (Hz)*	24038.46	*Solvent*	CHLOROFORM-d		
Spectrum Offset (Hz)	10046.3408	*Spectrum Type*	STANDARD	*Sweep Width (Hz)*	24037.73	*Temperature (degree C)*	25.008

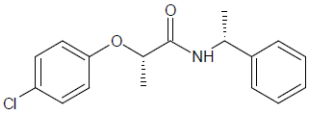

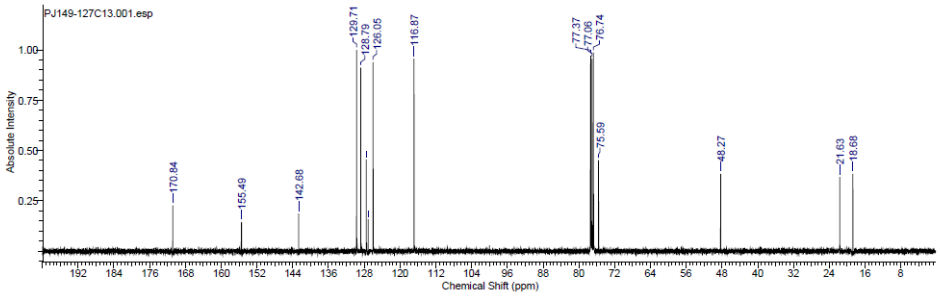

10/12/2017 11:29:54 AM
(2R)-2-(4-chlorophenoxy)-N-[(1R)-1-phenylethyl]propanamide

Acquisition Time (sec)	4.1069	*Comment*	Z116098_0411 (PA BBO 400S1 BBF-H-D-05 Z SP)	*Date*	27 Sep 2017 13:03:12
Date Stamp	27 Sep 2017 13:03:12		*File Name*	C:\Users\priya\Desktop\NMRSpectra\NMR#149\149FTD's\PJ149-129\1\fid	
Frequency (MHz)	399.54	*Nucleus*	1H	*Number of Transients*	16	*Origin*	spect
Original Points Count	32768	*Owner*	SMDC_A	*Points Count*	32768	*Pulse Sequence*	zg30
Receiver Gain	93.24	*SW(cyclical) (Hz)*	7978.72	*Solvent*	CHLOROFORM-d		
Spectrum Offset (Hz)	2467.1362	*Spectrum Type*	STANDARD	*Sweep Width (Hz)*	7978.48	*Temperature (degree C)*	24.999

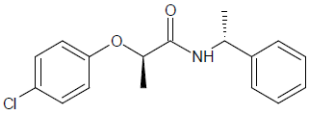

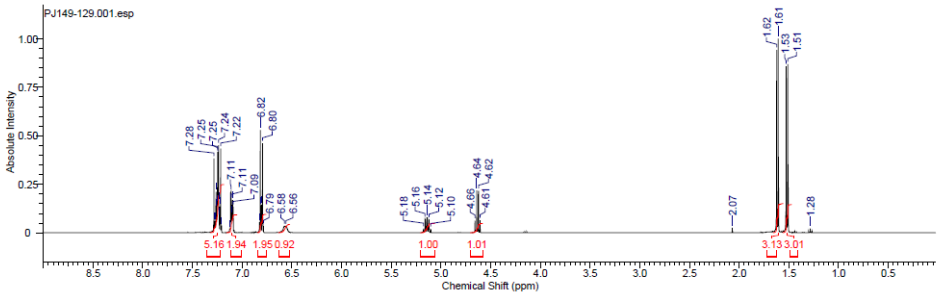

10/12/2017 12:26:50 PM
(2R)-2-(4-chlorophenoxy)-N-[(1R)-1-phenylethyl]propanamide

Acquisition Time (sec)	1.3631	*Comment*	Z116098_0411 (PA BBO 400S1 BBF-H-D-05 Z SP)			*Date*	27 Sep 2017 13:13:52
Date Stamp	27 Sep 2017 13:13:52			*File Name*	C:\Users\priya\Desktop\NMRSpectra\NMR#149\149FTD's\PJ149-129C13\2\fid		
Frequency (MHz)	100.46	*Nucleus*	13C	*Number of Transients*	131	*Origin*	spect
Original Points Count	32768	*Owner*	SMDC_A	*Points Count*	32768	*Pulse Sequence*	zgpg30
Receiver Gain	208.51	*SW(cyclical) (Hz)*	24038.46	*Solvent*	CHLOROFORM-d		
Spectrum Offset (Hz)	10046.3408	*Spectrum Type*	STANDARD	*Sweep Width (Hz)*	24037.73	*Temperature (degree C)*	24.999

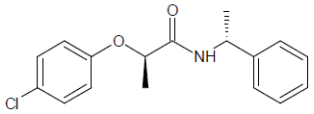

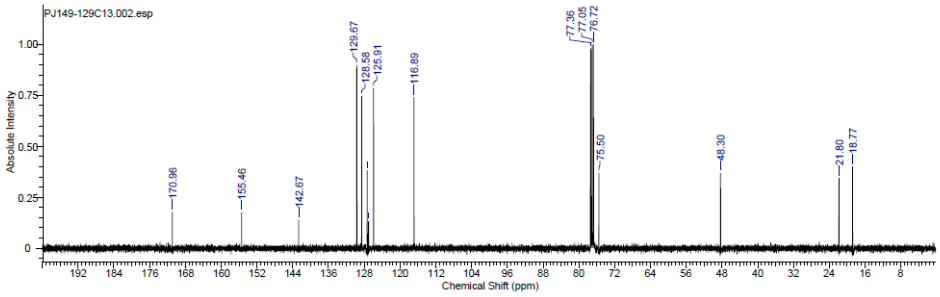

Sequences

> heIF2B1_alpha_codonopt

ATGGACGACAAAGAACTGATCGAATACTTCAAATCTCAGATGAAAGAAG
ACCCGGACATGGCTTCTGCTGTTGCTGCTATCCGTACCCTGCTGGAGTTCCTG
AAACGTGACAAAGGTGAAACCATCCAGGGTCTGCGTGCTAACCTGACCTCTG
CTATCGAAACCCTGTGCGGTGTTGACTCTTCTGTTGCTGTTTCTTCTGGTGGTG
AACTGTTCCTGCGTTTCATCTCTCTGGCTTCTCTGGAATACTCTGACTACTCTA
AATGCAAAAAAATCATGATCGAACGTGGTGAACTGTTCCTGCGTCGTATCTCT
CTGTCTCGTAACAAAATCGCTGACCTGTGCCACACCTTCATCAAAGACGGTG
CTACCATCCTGACCCACGCTTACTCTCGTGTTGTTCTGCGTGTTCTGGAAGCT
GCTGTTGCTGCTAAAAAACGTTTCTCTGTTTACGTTACCGAATCTCAGCCGGA
CCTGTCTGGTAAAAAAATGGCTAAAGCTCTGTGCCACCTGAACGTTCCGGTTA
CCGTTGTTCTGGACGCTGCTGTTGGTTACATCATGGAAAAAGCTGACCTGGTT
ATCGTTGGTGCTGAAGGTGTTGTTGAAAACGGTGGTATCATCAACAAAATCG
GTACCAACCAGATGGCTGTTTGCGCTAAAGCTCAGAACAAACCGTTCTACGT
TGTTGCTGAATCTTTCAAATTCGTTCGTCTGTTCCCGCTGAACCAGCAGGACG
TTCCGGACAAATTCAAATACAAAGCTGACACCCTGAAAGTTGCTCAGACCGG
TCAGGACCTGAAAGAAGAACACCCGTGGGTTGACTACACCGCTCCGTCTCTG
ATCACCCTGCTGTTCACCGACCTGGGTGTTCTGACCCCGTCTGCTGTTTCTGA
CGAACTGATCAAACTGTACCTGTAA

>heIF2B2_beta_codonopt | 6x His tag, TEV site

ATGCATCACCATCATCACCACGGTGGTGGTTCTGAAAACCTGTACTTCCA
GTCTCCGGGTTCTGCTGCTAAAGGTTCTGAACTGTCTGAACGTATCGAATCTT
TCGTTGAAACCCTGAAACGTGGTGGTGGTCCGCGTTCTTCTGAAGAAATGGCT
CGTGAAACCCTGGGTCTGCTGCGTCAGATCATCACCGACCACCGTTGGTCTA
ACGCTGGTGAACTGATGGAACTGATCCGTCGTGAAGGTCGTCGTATGACCGC
TGCTCAGCCGTCTGAAACCACCGTTGGTAACATGGTTCGTCGTGTTCTGAAAA
TCATCCGTGAAGAATACGGTCGTCTGCACGGTCGTTCTGACGAATCTGACCA
GCAGGAATCTCTGCACAAACTGCTGACCTCTGGTGGTCTGAACGAAGACTTC
TCTTTCCACTACGCTCAGCTGCAGTCTAACATCATCGAAGCTATCAACGAACT
GCTGGTTGAACTGGAAGGTACGATGGAAAACATCGCTGCTCAGGCTCTGGAA
CACATCCACTCTAACGAAGTTATCATGACCATCGGTTTCTCTCGTACCGTTGA
AGCTTTCCTGAAAGAAGCTGCTCGTAAACGTAAATTCCACGTTATCGTTGCTG
AATGCGCTCCGTTCTGCCAGGGTCACGAAATGGCTGTTAACCTGTCTAAAGCT
GGTATCGAAACCACCGTTATGACCGACGCTGCTATCTTCGCTGTTATGTCTCG
TGTTAACAAAGTTATCATCGGTACCAAAACCATCCTGGCTAACGGTGCTCTGC
GTGCTGTTACCGGTACCCACACCCTGGCTCTGGCTGCTAAACACCACTCTACC
CCGCTGATCGTTTGCGCTCCGATGTTCAAACTGTCTCCGCAGTTCCCGAACGA
AGAAGACTCTTTCCACAAATTCGTTGCTCCGGAAGAAGTTCTGCCGTTCACCG
AAGGTGACATCCTGGAAAAAGTTTCTGTTCACTGCCCGGTTTTCGACTACGTT
CCGCCGGAACTGATCACCCTGTTCATCTCTAACATCGGTGGTAACGCTCCGTC
TTACATCTACCGTCTGATGTCTGAACTGTACCACCCGGACGACCACGTTCTGT
AA

>heIF2B3_gamma_codonopt

ATGGAGTTCCAGGCTGTTGTTATGGCTGTTGGTGGTGGTTCTCGTATGAC
CGACCTGACCTCTTCTATCCCGAAACCGCTGCTGCCGGTTGGTAACAAACCGC
TGATCTGGTACCCGCTGAACCTGCTGGAACGTGTTGGTTTCGAAGAAGTTATC
GTTGTTACCACCCGTGACGTTCAGAAAGCTCTGTGCGCTGAGTTCAAAATGA
AAATGAAACCGGACATCGTTTGCATCCCGGACGACGCTGACATGGGTACCGC
TGACTCTCTGCGTTACATCTACCCGAAACTGAAAACCGACGTTCTGGTTCTGT
CTTGCGACCTGATCACCGACGTTGCTCTGCACGAAGTTGTTGACCTGTTCCGT
GCTTACGACGCTTCTCTGGCTATGCTGATGCGTAAAGGTCAGGACTCTATCGA
ACCGGTTCCGGGTCAGAAAGGTAAAAAAAAAAGCTGTTGAACAGCGTGACTTC
ATCGGTGTTGACTCTACCGGTAAACGTCTGCTGTTCATGGCTAACGAAGCTGA
CCTGGACGAAGAACTGGTTATCAAAGGTTCTATCCTGCAGAAACACCCGCGT
ATCCGTTTCCACACCGGTCTGGTTGACGCTCACCTGTACTGCCTGAAAAAATA
CATCGTTGACTTCCTGATGGAAAACGGTTCTATCACCTCTATCCGTTCTGAAC
TGATCCCGTACCTGGTTCGTAAACAGTTCTCTTCTGCTTCTTCTCAGCAGGGTC
AGGAAGAAAAAGAAGAAGACCTGAAAAAAAAAGAACTGAAATCTCTGGACA
TCTACTCTTTCATCAAAGAAGCTAACACCCTGAACCTGGCTCCGTACGACGCT
TGCTGGAACGCTTGCCGTGGTGACCGTTGGGAAGACCTGTCTCGTTCTCAGGT
TCGTTGCTACGTTCACATCATGAAAGAAGGTCTGTGCTCTCGTGTTTCTACCC
TGGGTCTGTACATGGAAGCTAACCGTCAGGTTCCGAAACTGCTGTCTGCTCTG
TGCCCGGAAGAACCGCCGGTTCACTCTTCTGCTCAGATCGTTTCTAAACACCT
GGTTGGTGTTGACTCTCTGATCGGTCCGGAAACCCAGATCGGTGAAAAATCTT
CTATCAAACGTTCTGTTATCGGTTCTTCTTGCCTGATCAAAGACCGTGTTACC
ATCACCAACTGCCTGCTGATGAACTCTGTTACCGTTGAAGAAGGTTCTAACAT
CCAGGGTTCTGTTATCTGCAACAACGCTGTTATCGAAAAAGGTGCTGACATC
AAAGACTGCCTGATCGGTTCTGGTCAGCGTATCGAAGCTAAAGCTAAACGTG
TTAACGAAGTTATCGTTGGTAACGACCAGCTGATGGAAATCTAA

>heIF2B4_delta_codonopt | isoform 2

ATGGCTGCTGTTGCTGTTGCTGTTCGTGAAGACTCTGGTTCTGGTATGAA
AGCTGAACTGCCGCCGGGTCCGGGTGCTGTTGGTCGTGAAATGACCAAAGAA
GAAAAACTGCAGCTGCGTAAAGAAAAAAAACAGCAGAAAAAAAAACGTAAA
GAAGAAAAAGGTGCTGAACCGGAAACCGGTTCTGCTGTTTCTGCTGCTCAGT
GCCAGGTTGGTCCGACCCGTGAACTGCCGGAATCTGGTATCCAGCTGGGTAC
CCCGCGTGAAAAAGTTCCGGCTGGTCGTTCTAAAGCTGAACTGCGTGCTGAA
CGTCGTGCTAAACAGGAAGCTGAACGTGCTCTGAAACAGGCTCGTAAAGGTG
AACAGGGTGGTCCGCCGCCGAAAGCTTCTCCGTCTACCGCTGGTGAAACCCC
GTCTGGTGTTAAACGTCTGCCGGAATACCCGCAGGTTGACGACCTGCTGCTGC
GTCGTCTGGTTAAAAAACCGGAACGTCAGCAGGTTCCGACCCGTAAAGACTA
CGGTTCTAAAGTTTCTCTGTTCTCTCACCTGCCGCAGTACTCTCGTCAGAACTC
TCTGACCCAGTTCATGTCTATCCCGTCTTCTGTTATCCACCCGGCTATGGTTCG
TCTGGGTCTGCAGTACTCTCAGGGTCTGGTTTCTGGTTCTAACGCTCGTTGCA
TCGCTCTGCTGCGTGCTCTGCAGCAGGTTATCCAGGACTACACCACCCCGCCG
AACGAAGAACTGTCTCGTGACCTGGTTAACAAACTGAAACCGTACATGTCTT
TCCTGACCCAGTGCCGTCCGCTGTCTGCTTCTATGCACAACGCTATCAAATTC
CTGAACAAAGAAATCACCTCTGTTGGTTCTTCTAAACGTGAAGAAGAAGCTA

AATCTGAACTGCGTGCTGCTATCGACCGTTACGTTCAGGAAAAAATCGTTCTG
GCTGCTCAGGCTATCTCTCGTTTCGCTTACCAGAAAATCTCTAACGGTGACGT
TATCCTGGTTTACGGTTGCTCTTCTCTGGTTTCTCGTATCCTGCAGGAAGCTTG
GACCGAAGGTCGTCGTTTCCGTGTTGTTGTTGTTGACTCTCGTCCGTGGCTGG
AAGGTCGTCACACCCTGCGTTCTCTGGTTCACGCTGGTGTTCCGGCTTCTTAC
CTGCTGATCCCGGCTGCTTCTTACGTTCTGCCGGAAGTTTCTAAAGTTCTGCT
GGGTGCTCACGCTCTGCTGGCTAACGGTTCTGTTATGTCTCGTGTTGGTACCG
CTCAGCTGGCTCTGGTTGCTCGTGCTCACAACGTTCCGGTTCTGGTTTGCTGC
GAAACCTACAAATTCTGCGAACGTGTTCAGACCGACGCTTTCGTTTCTAACGA
ACTGGACGACCCGGACGACCTGCAGTGCAAACGTGGTGAACACGTTGCTCTG
GCTAACTGGCAGAACCACGCTTCTCTGCGTCTGCTGAACCTGGTTTACGACGT
TACCCCGCCGGAACTGGTTGACCTGGTTATCACCGAACTGGGTATGATCCCGT
GCTCTTCTGTTCCGGTTGTTCTGCGTGTTAAATCTTCTGACCAGTAA

>heIF2B5_epsilon1_codonopt | overlap
ATGGCTGCTCCGGTTGTTGCTCCGCCGGGTGTTGTTGTTTCTCGTGCTAAC
AAACGTTCTGGTGCTGGTCCGGGTGGTTCTGGTGGTGGTGGTGCTCGTGGTGC
TGAAGAAGAACCGCCGCCGCCGCTGCAGGCTGTTCTGGTTGCTGACTCTTTCG
ACCGTCGTTTCTTCCCGATCTCTAAAGACCAGCCGCGTGTTCTGCTGCCGCTG
GCTAACGTTGCTCTGATCGACTACACCCTGGAGTTCCTGACCGCTACCGGTGT
TCAGGAAACCTTCGTTTTCTGCTGCTGGAAAGCTGCTCAGATCAAAGAACAC
CTGCTGAAATCTAAATGGTGCCGTCCGACCTCTCTGAACGTTGTTCGTATCAT
CACCTCTGAACTGTACCGTTCTCTGGGTGACGTTCTGCGTGACGTTGACGCTA
AAGCTCTGGTTCGTTCTGACTTCCTGCTGGTTTACGGTGACGTTATCTCTAAC
ATCAACATCACCCGTGCTCTGGAAGAACACCGTCTGCGTCGTAAACTGGAAA
AAAACGTTTCTGTTATGACCATGATCTTCAAAGAATCTTCTCCGTCTCACCCG
ACCCGTTGCCACGAAGACAACGTTGTTGTTGCTGTTGACTCTACCACCAACCG
TGTTCTGCACTTCCAGAAAACCCAGGGTCTGCGTCGTTTCGCTTTCCCGCTGT
CTCTGTTCCAGGGTTCTTCTGACGGTGTTGAAGTTCGTTACGACCTGCTGGAC
TGCCACATCTCTATCTGCTCTCCGCAGGTTGCTCAGCTGTTCACCGACAACTT
CGACTACCAGACCCGTGACGACTTCGTTCGTGGTCTGCTGGTTAACGAAGAA
ATCCTGGGTAACCAGATCCACATGCACGTTACCGCTAAAGAATACGGTGCTC
GTGTTTCTAACCTGCACATGTACTCTGCTGTTTGCGCTGACGTTATCCGTCGTT
GGGTTTACCCGCTGACCCCGGAAGCTAACTTCACCGACTCTACCACCCAGTCT
TGCACCCACTCTCGTCACAACATCTACCGTGGTCCGGAAGTTTCTCTGGGTCA
CGGTTCTATCCTGGAAGAAAACGTTCTGCTGGGTTCTGGTACCGTT

>heIF2B5_epsilon2_codonopt | overlap
CTGCTGGGTTCTGGTACCGTTATCGGTTCTAACTGCTTCATCACCAACTCT
GTTATCGGTCCGGGTTGCCACATCGGTGACAACGTTGTTCTGGACCAGACCTA
CCTGTGGCAGGGTGTTCGTGTTGCTGCTGGTGCTCAGATCCACCAGTCTCTGC
TGTGCGACAACGCTGAAGTTAAAGAACGTGTTACCCTGAAACCGCGTTCTGT
TCTGACCTCTCAGGTTGTTGTTGGTCCGAACATCACCCTGCCGGAAGGTTCTG
TTATCTCTCTGCACCCGCCGGACGCTGAAGAAGACGAAGACGACGGTGAGTT
CTCTGACGACTCTGGTGCTGACCAGGAAAAAGACAAAGTTAAAATGAAAGGT
TACAACCCGGCTGAAGTTGGTGCTGCTGGTAAAGGTTACCTGTGGAAAGCTG

CTGGTATGAACATGGAAGAAGAAGAAGAACTGCAGCAGAACCTGTGGGGTC
TGAAAATCAACATGGAAGAAGAATCTGAATCTGAATCTGAACAGTCTATGGA
CTCTGAAGAACCGGACTCTCGTGGTGGTTCTCCGCAGATGGACGACATCAAA
GTTTTCCAGAACGAAGTTCTGGGTACCCTGCAGCGTGGTAAAGAAGAAAACA
TCTCTTGCGACAACCTGGTTCTGGAAATCAACTCTCTGAAATACGCTTACAAC
GTTTCTCTGAAAGAAGTTATGCAGGTTCTGTCTCACGTTGTTCTGGAGTTCCC
GCTGCAGCAGATGGACTCTCCGCTGGACTCTTCTCGTTACTGCGCTCTGCTGC
TGCCGCTGCTGAAAGCTTGGTCTCCGGTTTTCCGTAACTACATCAAACGTGCT
GCTGACCACCTGGAAGCTCTGGCTGCTATCGAAGACTTCTTCCTGGAACACG
AAGCTCTGGGTATCTCTATGGCTAAAGTTCTGATGGCTTTCTACCAGCTGGAA
ATCCTGGCTGAAGAAACCATCCTGTCTTGGTTCTCTCAGCGTGACACCACCGA
CAAAGGTCAGCAGCTGCGTAAAAACCAGCAGCTGCAGCGTTTCATCCAGTGG
CTGAAAGAAGCTGAAGAAGAATCTTCTGAAGACGACTAA

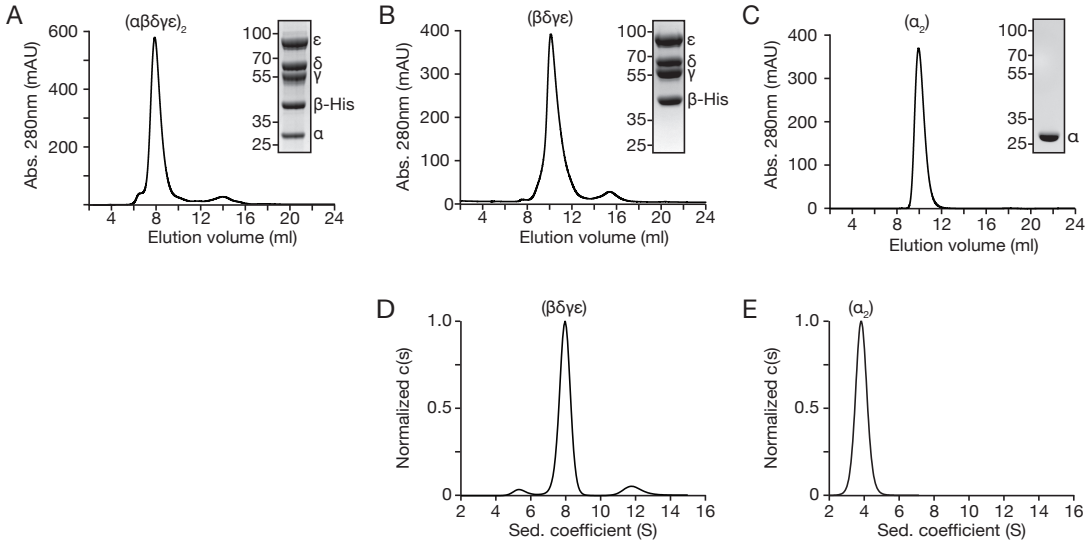

Fig. S1

Purification and characterization of decameric eIF2B. Characterization of (A) eIF2B$(\alpha\beta\gamma\delta\varepsilon)_2$, (B) eIF2B$(\beta\gamma\delta\varepsilon)$, and (C) eIF2B$(\alpha_2)$, by size-exclusion chromatography. Peak fractions were concentrated and characterized further by SDS-PAGE followed by Coomassie blue staining. Characterization of (D) eIF2B$(\alpha\beta\gamma\delta\varepsilon)_2$ and (E) eIF2B(α_2) by analytical ultracentrifugation.

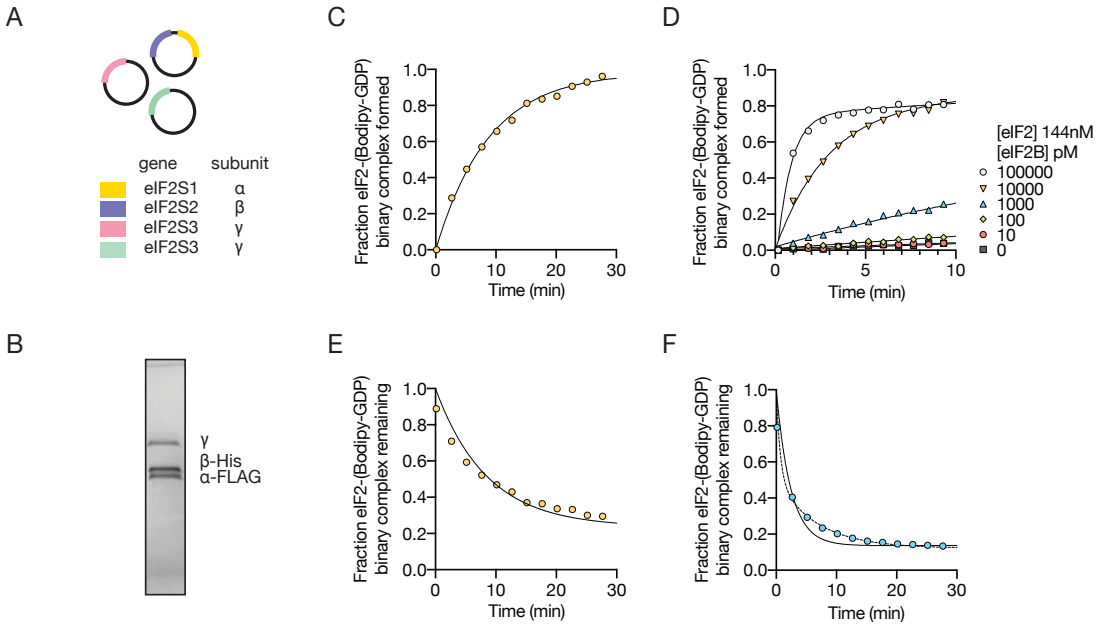

Fig. S2

Purification of substrate eIF2 and implementation of GDP exchange assay. (A) Recombinant *S. cerevisiae* expression system for human eIF2 as described in (*30*). Two copies of eIF2γ compensate for low expression of this gene. (B) Characterization of purified eIF2 by SDS-PAGE followed by Coomassie blue staining. (C) Fluorescent GDP loading and subsequent (D) unloading curves in the presence of 10 nM eIF2B. (E) GEF activity varies with eIF2B$(\alpha\beta\gamma\delta\varepsilon)_2$ concentration as measured by loading of fluorescent GDP. (F) Comparison of single-(solid line) and double-exponential (dotted line) fits of ISRIB-mediated GDP unloading. Double-exponential fits correlate better with the data (R^2 = 0.98 for double, 0.88 for single) but cannot be explained by current models for nucleotide exchange.

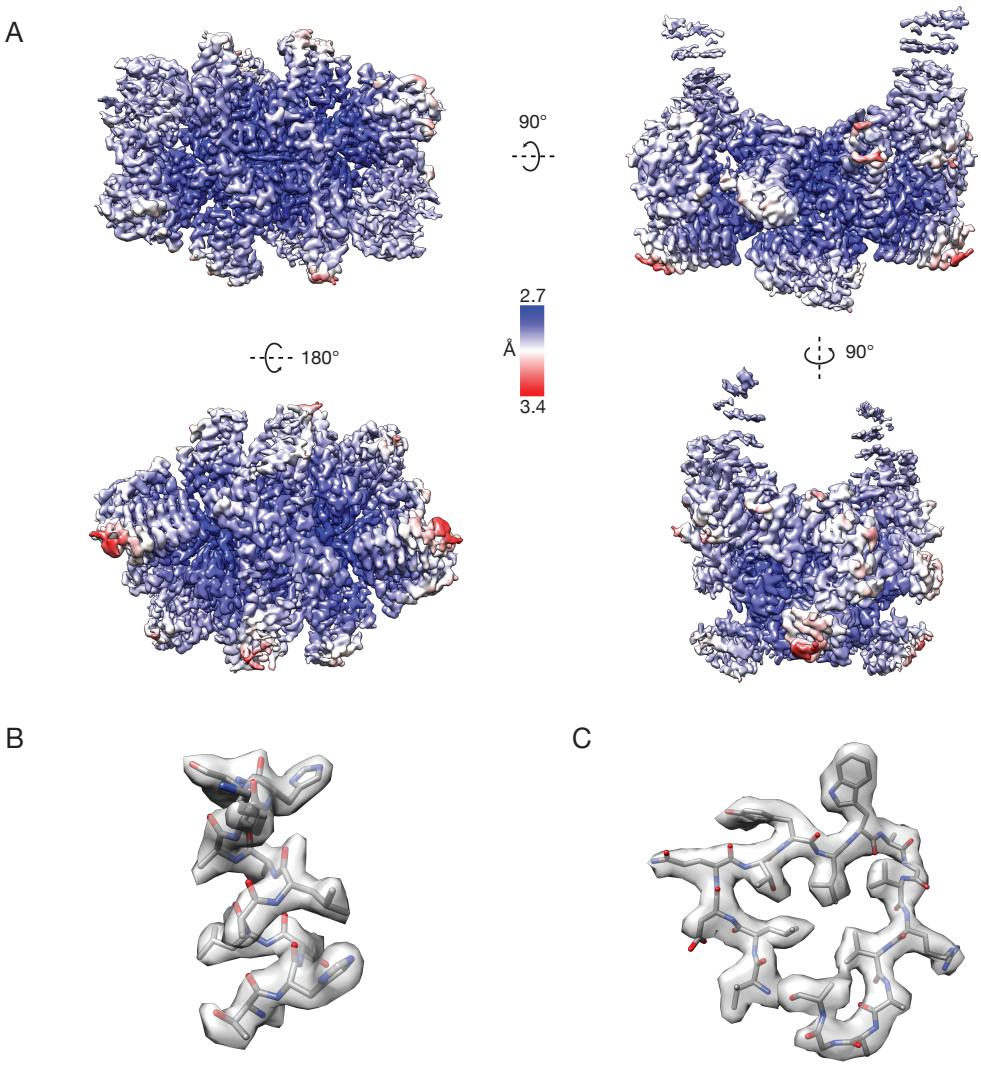

Fig. S3

Local resolution. (A) Local resolution estimates determined using RELION 2.1 and displayed using UCSF Chimera. Superlative regions of the cryoEM map rendered as a transparent isosurface and interpreted with atomic coordinates for an (B) alpha-helix and a turn of a (C) beta-solenoid.

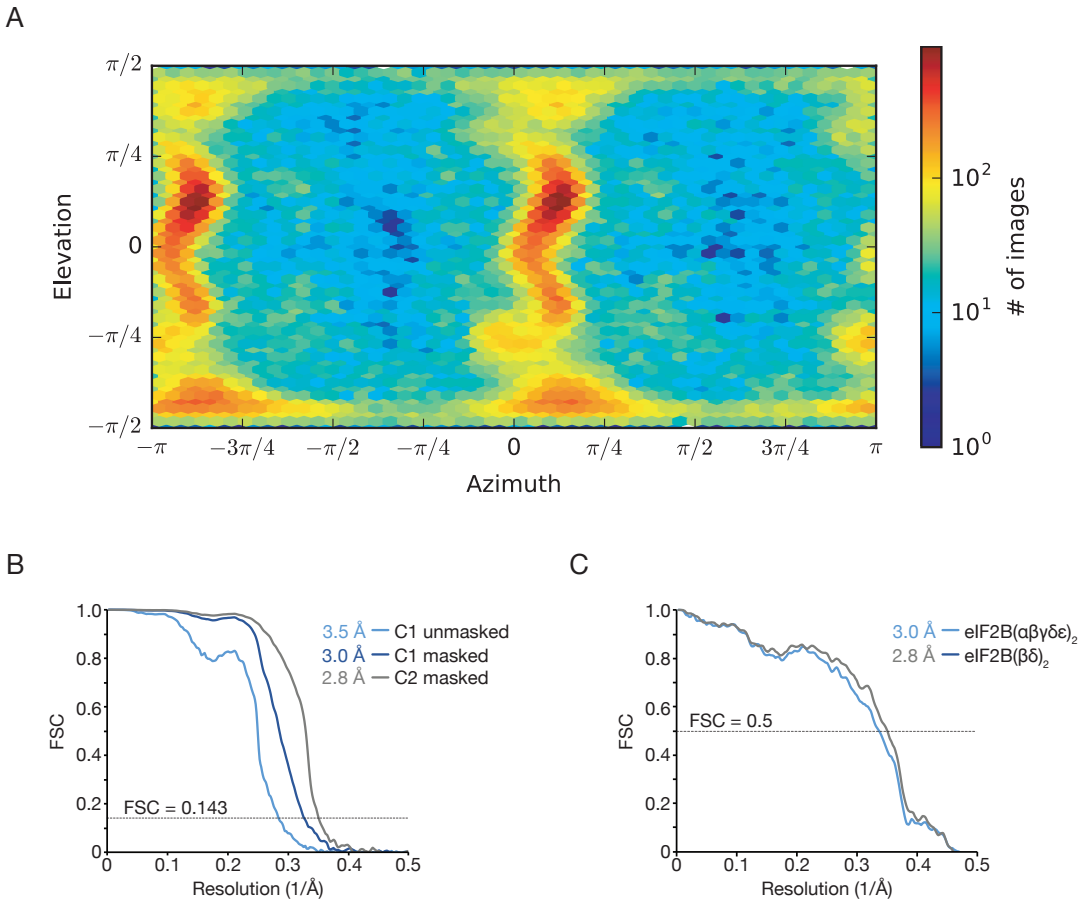

Fig. S4

Particle orientation distribution and resolution determination. (A) Plot of per-particle direction distribution over azimuth and elevation angles using CryoSPARC. (B) Fourier shell correlations for independent half maps reconstructed without symmetry or masking, versus without symmetry and with soft masking, and versus with C2 symmetry and soft masking. (C) Fourier shell correlations for the final cryoEM density map versus simulated density maps for the atomic model of the intact decamer versus the ISRIB-stabilized subunits alone.

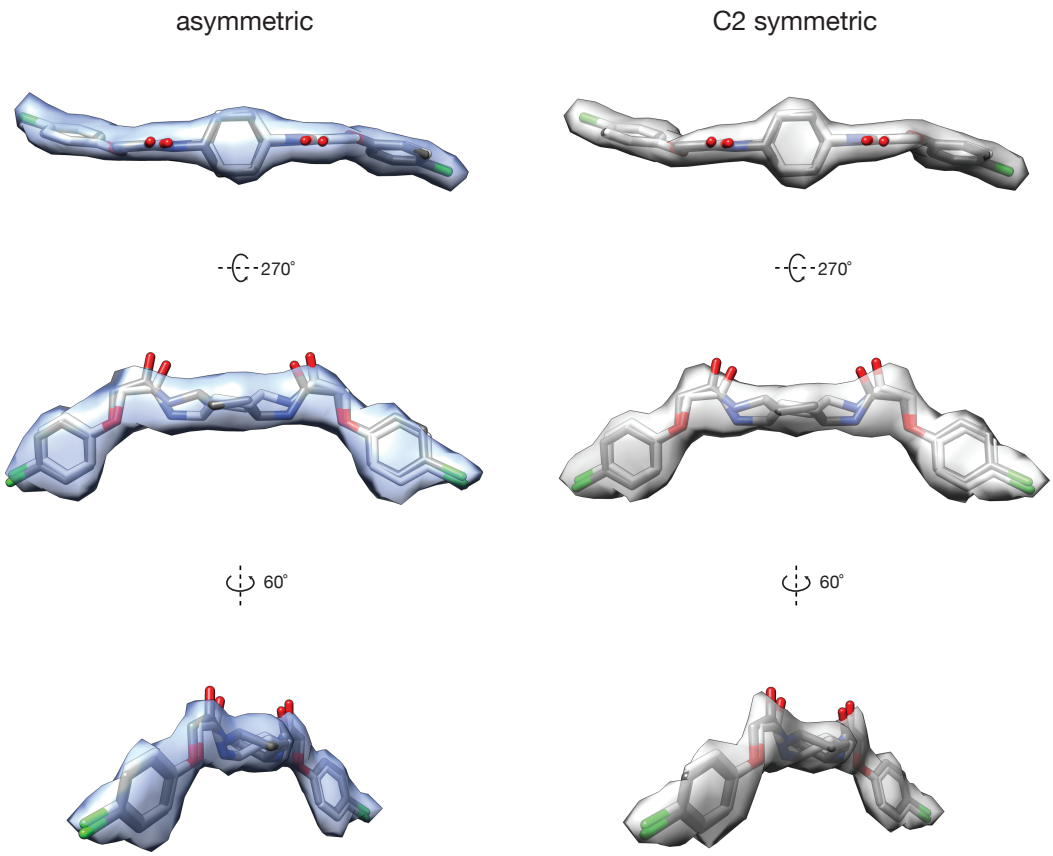

Fig. S5

Symmetry and multiple conformer interpretation of the ligand density. Isosurface representations of the cryoEM density computed without symmetry (left, blue) versus with C2 symmetry imposed throughout refinement (right, gray). Although additional conformers of the ligand remain possible given the density, the pair of chair conformers shown are related by rotations of 180º about the N–C bonds to the central cyclohexane ring, or equivalently by rotation of the entire ligand 180º about the axis orthogonal to the plane of the cyclohexane ring. The U-shaped conformation of the O-arylglycolamide side chains is consistent with extensive structure–activity studies of ISRIB analogs (see Fig. S6, (*28*, *34*))

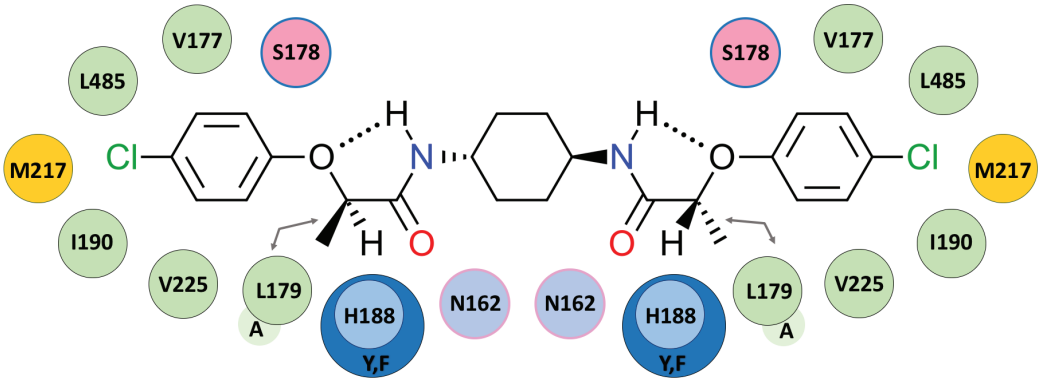

Fig. S6

ISRIB binding environment and key mutants. A subset of residues lining the ISRIB binding pocket are rendered as bubbles and color-coded according to amino acid properties. βM217 (yellow) contributes to the hydrophobicity of the pocket and an apparent sulfur-halogen interaction. βI190, βV225, δL485, δV177 and δL179 (green) contribute to the hydrophobicity of deep pockets in the binding site. Mutagenizing δL179 to Ala (smaller, lighter green circle) opened the binding pocket and enabled the methyl-substituted ISRIB-A19(*R,R*) analog to bind (arrows point to the mutated residue and the added methyl group, also see Figs. 2F and 5D). βN162 (blue), δS178 (pink), and βH188 (blue) coordinate polar moieties on ISRIB. Mutagenizing βH188 to more electron-rich aromatic residues, Tyr or Phe, (larger, darker blue circle), enhanced ISRIB binding, consistent with a stronger C-H-π interaction in the mutants (also see Figs. 2F, Fig. 3). The proposed upside-down "U-shaped" conformation of the ligand may be stabilized by weak intramolecular hydrogen bonds shown as dashed lines.

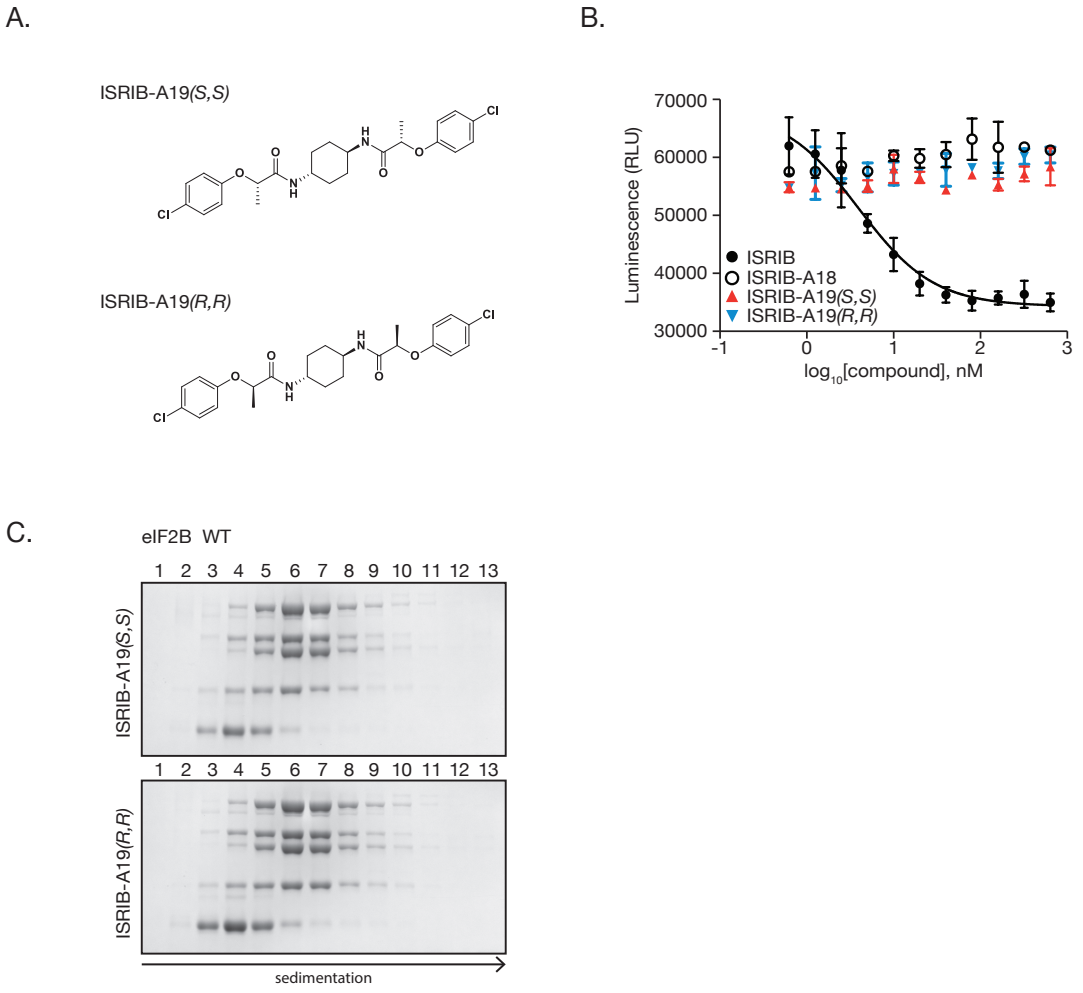

Fig. S7

Characterization of ISRIB-A19 enantiomers A19*(R,R)* and A19*(S,S)*. (A) Chemical structure of ISRIB-A19*(R,R)* and ISRIB-A19*(S,S)*. (B) Cell-based ATF4-luciferase assay with ISRIB, a previously characterized inactive analog ISRIB-A18 (*28*), ISRIB-A19*(R,R)*, and ISRIB-*A19(S,S)* (n = 3). ISRIB was measured to have an EC_{50} of 3.94 nM for reversal of tunicamycin induced ATF-luciferase production. (C) Stability of eIF2B$(\alpha\beta\gamma\delta\varepsilon)_2$ in the presence of 500 nM ISRIB-A19*(R,R)* or ISRIB-*A19(S,S)* as assessed by velocity sedimentation on sucrose gradients.

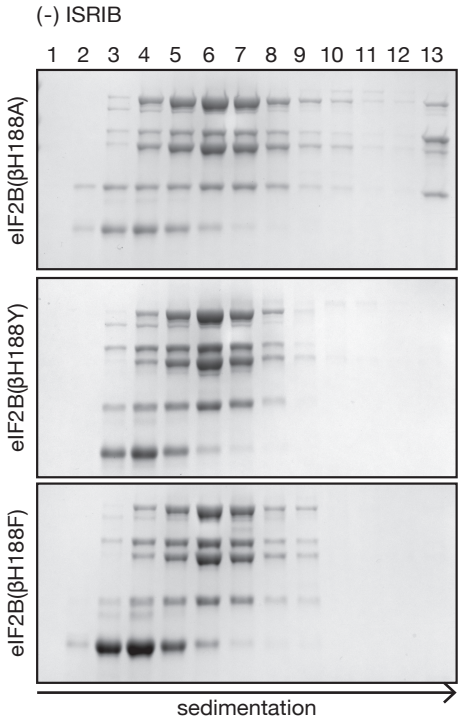

Fig. S8

Characterization of βH188 mutations by sedimentation velocity. Stability of eIF2B$(\alpha\beta\gamma\delta\varepsilon)_2$ in the context of βH188A, βH188Y, and βH188F mutations as assessed by velocity sedimentation on sucrose gradients in the absence of ISRIB.

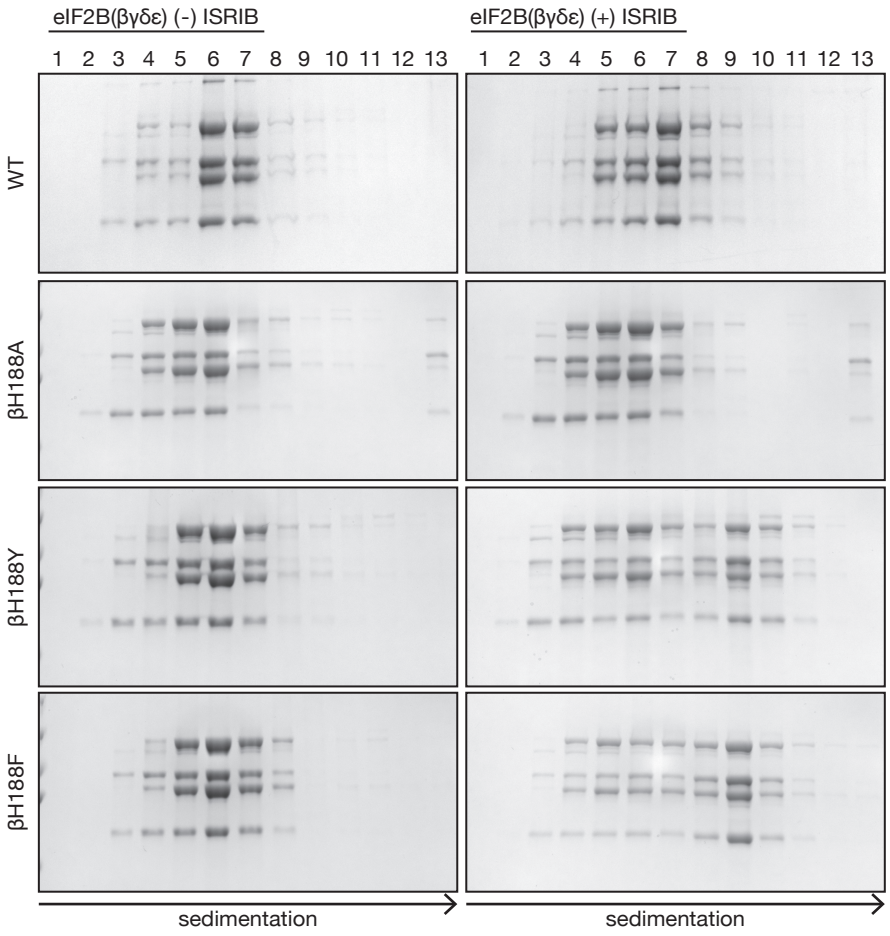

Fig. S9

eIF2B(βγδε) mutants enhance ISRIB-mediated dimerization. Stability of eIF2B$(\beta\gamma\delta\varepsilon)_2$ in the context of wild-type, βH188A, βH188Y, and βH188F as assessed by velocity sedimentation on sucrose gradients in the presence and absence of ISRIB.

Table S1.
Data Collection Parameters

Data Collection				
	$eIF2B(\alpha\beta\gamma\delta\varepsilon)_2$ + ISRIB at Janelia	$eIF2B(\alpha\beta\gamma\delta\varepsilon)_2$ + ISRIB at Berkeley	$eIF2B(\alpha\beta\gamma\delta)$	$eIF2B(\alpha\beta\gamma\delta)$ + ISRIB
Pixel Size (Å)	1.02	0.838	1.15	1.15
Defocus Range (microns)	-0.3 to -3.9	-0.3 to -3.9	-0.7 to -5.5	-0.6 to -5.4
Defocus Mean (microns)	-2.0	-1.8	-1.9	-1.8
Voltage (kV)	300	300	200	200
Magnification (x)	29,000	29,000	36,000	36,000
Spherical Aberration (mm)	2.7	2.62	2.0	2.0
Detector	K2 Summit	K2 Summit	K2 Summit	K2 Summit
Detector Pixel Size (microns)	5.0	5.0	5.0	5.0
Per frame electron dose ($e^-/Å^2$)	1.19	1.63	1.2	1.2
# of frames	67	27	40	40
Frame Length (seconds)	0.15	0.18	0.2	0.2
Micrographs	1780	1515	129	67

Table S2.
Refinement Parameters

Refinement			
	eIF2B(αβγδε)$_2$ + ISRIB at Janelia	eIF2B(αβγδε)$_2$ + ISRIB at Berkeley	Combined
Particles following 2D classification	102599	99526	202,125
FSC Average Resolution, unmasked (Å)	3.8	3.5	3.0
FSC Average Resolution, masked (Å)	3.4	3.2	2.8
Map Sharpening B-factor	-75	-75	-78

Table S3
Modeling

Model Statistics	
Number of Atoms, macromolecules	24208
Number of Atoms, ligands	60
Molprobity Score	1.62
Clashscore, all atoms	5.56
Favored Rotamers (%)	99.76
Outlier Rotamers (%)	0.24
RMS (bonds)	0.0047
RMS (angles)	1.16
Ramachandran Favored (%)	95.43
Ramachandran Outliers (%)	0.00
Ramachandran Allowed (%)	4.57

References

1. R. P. Dalton, D. B. Lyons, S. Lomvardas, Co-opting the unfolded protein response to elicit olfactory receptor feedback. *Cell* **155**, 321–332 (2013). doi:10.1016/j.cell.2013.09.033 Medline

2. M. Costa-Mattioli, D. Gobert, H. Harding, B. Herdy, M. Azzi, M. Bruno, M. Bidinosti, C. Ben Mamou, E. Marcinkiewicz, M. Yoshida, H. Imataka, A. C. Cuello, N. Seidah, W. Sossin, J.-C. Lacaille, D. Ron, K. Nader, N. Sonenberg, Translational control of hippocampal synaptic plasticity and memory by the eIF2α kinase GCN2. *Nature* **436**, 1166–1173 (2005). doi:10.1038/nature03897 Medline

3. D. H. Munn, M. D. Sharma, B. Baban, H. P. Harding, Y. Zhang, D. Ron, A. L. Mellor, GCN2 kinase in T cells mediates proliferative arrest and anergy induction in response to indoleamine 2,3-dioxygenase. *Immunity* **22**, 633–642 (2005). doi:10.1016/j.immuni.2005.03.013 Medline

4. N. C. Wortham, M. Martinez, Y. Gordiyenko, C. V. Robinson, C. G. Proud, Analysis of the subunit organization of the eIF2B complex reveals new insights into its structure and regulation. *FASEB J.* **28**, 2225–2237 (2014). doi:10.1096/fj.13-243329 Medline

5. Y. Gordiyenko, C. Schmidt, M. D. Jennings, D. Matak-Vinkovic, G. D. Pavitt, C. V. Robinson, eIF2B is a decameric guanine nucleotide exchange factor with a γ2ε2 tetrameric core. *Nat. Commun.* **5**, 3902 (2014). doi:10.1038/ncomms4902 Medline

6. A. M. Bogorad, B. Xia, D. G. Sandor, A. B. Mamonov, T. R. Cafarella, S. Jehle, S. Vajda, D. Kozakov, A. Marintchev, Insights into the architecture of the eIF2Bα/β/δ regulatory subcomplex. *Biochemistry* **53**, 3432–3445 (2014). Medline

7. B. Kuhle, N. K. Eulig, R. Ficner, Architecture of the eIF2B regulatory subcomplex and its implications for the regulation of guanine nucleotide exchange on eIF2. *Nucleic Acids Res.* **43**, 9994–10014 (2015). Medline

8. K. Kashiwagi, M. Takahashi, M. Nishimoto, T. B. Hiyama, T. Higo, T. Umehara, K. Sakamoto, T. Ito, S. Yokoyama, Crystal structure of eukaryotic translation initiation factor 2B. *Nature* **531**, 122–125 (2016). doi:10.1038/nature16991 Medline

9. E. Gomez, S. S. Mohammad, G. D. Pavitt, Characterization of the minimal catalytic domain within eIF2B: The guanine-nucleotide exchange factor for translation initiation. *EMBO J.* **21**, 5292–5301 (2002). doi:10.1093/emboj/cdf515 Medline

10. W. Yang, A. G. Hinnebusch, Identification of a regulatory subcomplex in the guanine nucleotide exchange factor eIF2B that mediates inhibition by phosphorylated eIF2. *Mol. Cell. Biol.* **16**, 6603–6616 (1996). doi:10.1128/MCB.16.11.6603 Medline

11. G. D. Pavitt, K. V. Ramaiah, S. R. Kimball, A. G. Hinnebusch, eIF2 independently binds two distinct eIF2B subcomplexes that catalyze and regulate guanine-nucleotide exchange. *Genes Dev.* **12**, 514–526 (1998). doi:10.1101/gad.12.4.514 Medline

12. T. Krishnamoorthy, G. D. Pavitt, F. Zhang, T. E. Dever, A. G. Hinnebusch, Tight binding of the phosphorylated α subunit of initiation factor 2 (eIF2α) to the regulatory subunits of guanine nucleotide exchange factor eIF2B is required for inhibition of translation initiation. *Mol. Cell. Biol.* **21**, 5018–5030 (2001). doi:10.1128/MCB.21.15.5018-5030.2001 Medline

13. A. G. Hinnebusch, J. R. Lorsch, The mechanism of eukaryotic translation initiation: New insights and challenges. *Cold Spring Harb. Perspect. Biol.* **4**, a011544 (2012). doi:10.1101/cshperspect.a011544 Medline

14. A. G. Hinnebusch, The scanning mechanism of eukaryotic translation initiation. *Annu. Rev. Biochem.* **83**, 779–812 (2014). doi:10.1146/annurev-biochem-060713-035802 Medline

15. H. P. Harding, I. Novoa, Y. Zhang, H. Zeng, R. Wek, M. Schapira, D. Ron, Regulated translation initiation controls stress-induced gene expression in mammalian cells. *Mol. Cell* **6**, 1099–1108 (2000). doi:10.1016/S1097-2765(00)00108-8 Medline

16. K. M. Vattem, R. C. Wek, Reinitiation involving upstream ORFs regulates ATF4 mRNA translation in mammalian cells. *Proc. Natl. Acad. Sci. U.S.A.* **101**, 11269–11274 (2004). doi:10.1073/pnas.0400541101 Medline

17. H. P. Harding, Y. Zhang, H. Zeng, I. Novoa, P. D. Lu, M. Calfon, N. Sadri, C. Yun, B. Popko, R. Paules, D. F. Stojdl, J. C. Bell, T. Hettmann, J. M. Leiden, D. Ron, An integrated stress response regulates amino acid metabolism and resistance to oxidative stress. *Mol. Cell* **11**, 619–633 (2003). doi:10.1016/S1097-2765(03)00105-9 Medline

18. C. Sidrauski, D. Acosta-Alvear, A. Khoutorsky, P. Vedantham, B. R. Hearn, H. Li, K. Gamache, C. M. Gallagher, K. K.-H. Ang, C. Wilson, V. Okreglak, A. Ashkenazi, B. Hann, K. Nader, M. R. Arkin, A. R. Renslo, N. Sonenberg, P. Walter, Pharmacological brake-release of mRNA translation enhances cognitive memory. *eLife* **2**, e00498 (2013). doi:10.7554/eLife.00498 Medline

19. C. Sidrauski, A. M. McGeachy, N. T. Ingolia, P. Walter, The small molecule ISRIB reverses the effects of eIF2α phosphorylation on translation and stress granule assembly. *eLife* **4**, (2015). doi:10.7554/eLife.05033

20. G. V. Di Prisco, W. Huang, S. A. Buffington, C.-C. Hsu, P. E. Bonnen, A. N. Placzek, C. Sidrauski, K. Krnjević, R. J. Kaufman, P. Walter, M. Costa-Mattioli, Translational control of mGluR-dependent long-term depression and object-place learning by eIF2α. *Nat. Neurosci.* **17**, 1073–1082 (2014). doi:10.1038/nn.3754 Medline

21. H. P. Harding, D. Ron, in *Translational Control in Biology and Medicine*, M. B. Mathews, N. Sonenberg, J. W. B. Hershey, Eds. (Cold Spring Harbor Laboratory Press, 2007), pp. 345–368.

22. P. Remondelli, M. Renna, The endoplasmic reticulum unfolded protein response in neurodegenerative disorders and its potential therapeutic significance. *Front. Mol. Neurosci.* **10**, 187 (2017). doi:10.3389/fnmol.2017.00187 Medline

23. J. Obacz, T. Avril, P.-J. Le Reste, H. Urra, V. Quillien, C. Hetz, E. Chevet, Endoplasmic reticulum proteostasis in glioblastoma—From molecular mechanisms to therapeutic perspectives. *Sci. Signal.* **10**, eaal2323 (2017). doi:10.1126/scisignal.aal2323

24. G. Martínez, C. Duran-Aniotz, F. Cabral-Miranda, J. P. Vivar, C. Hetz, Endoplasmic reticulum proteostasis impairment in aging. *Aging Cell* **16**, 615–623 (2017). doi:10.1111/acel.12599 Medline

25. P. A. J. Leegwater, G. Vermeulen, A. A. M. Könst, S. Naidu, J. Mulders, A. Visser, P. Kersbergen, D. Mobach, D. Fonds, C. G. M. van Berkel, R. J. L. F. Lemmers, R. R. Frants, C. B. M. Oudejans, R. B. H. Schutgens, J. C. Pronk, M. S. van der Knaap, Subunits of the translation initiation factor eIF2B are mutant in leukoencephalopathy with vanishing white matter. *Nat. Genet.* **29**, 383–388 (2001). doi:10.1038/ng764 Medline

26. M. Halliday, H. Radford, Y. Sekine, J. Moreno, N. Verity, J. le Quesne, C. A. Ortori, D. A. Barrett, C. Fromont, P. M. Fischer, H. P. Harding, D. Ron, G. R. Mallucci, Partial restoration of protein synthesis rates by the small molecule ISRIB prevents neurodegeneration without pancreatic toxicity. *Cell Death Dis.* **6**, e1672–e1679 (2015). doi:10.1038/cddis.2015.49 Medline

27. A. Chou, K. Krukowski, T. Jopson, P. J. Zhu, M. Costa-Mattioli, P. Walter, S. Rosi, Inhibition of the integrated stress response reverses cognitive deficits after traumatic brain injury. *Proc. Natl. Acad. Sci. U.S.A.* **114**, E6420–E6426 (2017). doi:10.1073/pnas.1707661114 Medline

28. C. Sidrauski, J. C. Tsai, M. Kampmann, B. R. Hearn, P. Vedantham, P. Jaishankar, M. Sokabe, A. S. Mendez, B. W. Newton, E. L. Tang, E. Verschueren, J. R. Johnson, N. J. Krogan, C. S. Fraser, J. S. Weissman, A. R. Renslo, P. Walter, Pharmacological dimerization and activation of the exchange factor eIF2B antagonizes the integrated stress response. *eLife* **4**, e07314 (2015). doi:10.7554/eLife.07314 Medline

29. Y. Sekine, A. Zyryanova, A. Crespillo-Casado, P. M. Fischer, H. P. Harding, D. Ron, Mutations in a translation initiation factor identify the target of a memory-enhancing compound. *Science* **348**, 1027–1030 (2015). doi:10.1126/science.aaa6986 Medline

30. R. A. de Almeida, A. Fogli, M. Gaillard, G. C. Scheper, O. Boesflug-Tanguy, G. D. Pavitt, A yeast purification system for human translation initiation factors eIF2 and eIF2Bε and

their use in the diagnosis of CACH/VWM disease. *PLOS ONE* **8**, e53958 (2013). doi:10.1371/journal.pone.0053958 Medline

31. A. G. Rowlands, R. Panniers, E. C. Henshaw, The catalytic mechanism of guanine nucleotide exchange factor action and competitive inhibition by phosphorylated eukaryotic initiation factor 2. *J. Biol. Chem.* **263**, 5526–5533 (1988). Medline

32. D. D. Williams, N. T. Price, A. J. Loughlin, C. G. Proud, Characterization of the mammalian initiation factor eIF2B complex as a GDP dissociation stimulator protein. *J. Biol. Chem.* **276**, 24697–24703 (2001). doi:10.1074/jbc.M011788200 Medline

33. B. L. Craddock, C. G. Proud, The α-subunit of the mammalian guanine nucleotide-exchange factor eIF-2B is essential for catalytic activity in vitro. *Biochem. Biophys. Res. Commun.* **220**, 843–847 (1996). doi:10.1006/bbrc.1996.0495 Medline

34. B. R. Hearn, P. Jaishankar, C. Sidrauski, J. C. Tsai, P. Vedantham, S. D. Fontaine, P. Walter, A. R. Renslo, Structure-activity studies of Bis-O-arylglycolamides: Inhibitors of the integrated stress response. *ChemMedChem* **11**, 870–880 (2016). doi:10.1002/cmdc.201500483 Medline

35. A. F. Zyryanova, F. Weis, A. Faille, A. Abo Alard, A. Crespillo-Casado, Y. Sekine, H. P. Harding, F. Allen, L. Parts, C. Fromont, P. M. Fischer, A. J. Warren, D. Ron, Binding of ISRIB reveals a regulatory site in the nucleotide exchange factor eIF2B. *Science* **359**, 1533 (2018).

36. S. Q. Zheng, E. Palovcak, J.-P. Armache, K. A. Verba, Y. Cheng, D. A. Agard, MotionCor2: Anisotropic correction of beam-induced motion for improved cryo-electron microscopy. *Nat. Methods* **14**, 331–332 (2017). doi:10.1038/nmeth.4193 Medline

37. K. Zhang, Gctf: Real-time CTF determination and correction. *J. Struct. Biol.* **193**, 1–12 (2016). doi:10.1016/j.jsb.2015.11.003 Medline

38. D. Kimanius, B. O. Forsberg, S. H. Scheres, E. Lindahl, Accelerated cryo-EM structure determination with parallelisation using GPUs in RELION-2. *eLife* **5**, e18722 (2016). doi:10.7554/eLife.18722 Medline

39. A. Punjani, J. L. Rubinstein, D. J. Fleet, M. A. Brubaker, cryoSPARC: Algorithms for rapid unsupervised cryo-EM structure determination. *Nat. Methods* **14**, 290–296 (2017). doi:10.1038/nmeth.4169 Medline

40. N. Grigorieff, Frealign: An exploratory tool for single-particle cryo-EM. *Methods Enzymol.* **579**, 191–226 (2016). doi:10.1016/bs.mie.2016.04.013 Medline

41. E. F. Pettersen, T. D. Goddard, C. C. Huang, G. S. Couch, D. M. Greenblatt, E. C. Meng, T. E. Ferrin, UCSF Chimera—a visualization system for exploratory research and analysis. *J. Comput. Chem.* **25**, 1605–1612 (2004). doi:10.1002/jcc.20084 Medline

42. L. A. Kelley, S. Mezulis, C. M. Yates, M. N. Wass, M. J. E. Sternberg, The Phyre2 web portal for protein modeling, prediction and analysis. *Nat. Protoc.* **10**, 845–858 (2015). doi:10.1038/nprot.2015.053 Medline

43. T. B. Hiyama, T. Ito, H. Imataka, S. Yokoyama, Crystal structure of the α subunit of human translation initiation factor 2B. *J. Mol. Biol.* **392**, 937–951 (2009). doi:10.1016/j.jmb.2009.07.054 Medline

44. N. W. Moriarty, R. W. Grosse-Kunstleve, P. D. Adams, Electronic Ligand Builder and Optimization Workbench (eLBOW): A tool for ligand coordinate and restraint generation. *Acta Crystallogr. D* **65**, 1074–1080 (2009). doi:10.1107/S0907444909029436 Medline

45. P. Emsley, B. Lohkamp, W. G. Scott, K. Cowtan, Features and development of Coot. *Acta Crystallogr. D* **66**, 486–501 (2010). doi:10.1107/S0907444910007493 Medline

46. P. D. Adams, P. V. Afonine, G. Bunkóczi, V. B. Chen, I. W. Davis, N. Echols, J. J. Headd, L.-W. Hung, G. J. Kapral, R. W. Grosse-Kunstleve, A. J. McCoy, N. W. Moriarty, R. Oeffner, R. J. Read, D. C. Richardson, J. S. Richardson, T. C. Terwilliger, P. H. Zwart, PHENIX: A comprehensive Python-based system for macromolecular structure solution. *Acta Crystallogr. D* **66**, 213–221 (2010). doi:10.1107/S0907444909052925 Medline

47. V. B. Chen, W. B. Arendall 3rd, J. J. Headd, D. A. Keedy, R. M. Immormino, G. J. Kapral, L. W. Murray, J. S. Richardson, D. C. Richardson, MolProbity: All-atom structure validation for macromolecular crystallography. *Acta Crystallogr. D* **66**, 12–21 (2010). doi:10.1107/S0907444909042073 Medline

48. S. J. Ludtke, Single-particle refinement and variability analysis in EMAN2.1. *Methods Enzymol.* **579**, 159–189 (2016). doi:10.1016/bs.mie.2016.05.001 Medline

49. P. Schuck, Size-distribution analysis of macromolecules by sedimentation velocity ultracentrifugation and lamm equation modeling. *Biophys. J.* **78**, 1606–1619 (2000). doi:10.1016/S0006-3495(00)76713-0 Medline